BJ www.biochemj.org

BJ Structure

Biochem. J. (2008) **415**, 429–437 (Printed in Great Britain) doi:10.1042/BJ20080569

Anti-cooperative assembly of the SRP19 and SRP68/72 components of the signal recognition particle

Tuhin Subhra MAITY*, Howard M. FRIED†[1] and Kevin M. WEEKS*[1]

*Department of Chemistry, University of North Carolina, Chapel Hill, NC 27599-3290, U.S.A., and †Department of Biochemistry and Biophysics, University of North Carolina, Chapel Hill, NC 27599-7260, U.S.A.

The mammalian SRP (signal recognition particle) represents an important model for the assembly and role of inter-domain interactions in complex RNPs (ribonucleoproteins). In the present study we analysed the interdependent interactions between the SRP19, SRP68 and SRP72 proteins and the SRP RNA. SRP72 binds the SRP RNA largely via non-specific electrostatic interactions and enhances the affinity of SRP68 for the RNA. SRP19 and SRP68 both bind directly and specifically to the same two RNA helices, but on opposite faces and at opposite ends. SRP19 binds at the apices of helices 6 and 8, whereas the SRP68/72 heterodimer binds at the three-way junction involving RNA helices 5, 6 and 8. Even though both SRP19 and SRP68/72 stabilize a similar parallel orientation for RNA helices 6 and 8, these two proteins bind to the RNA with moderate anti-co-operativity. Long-range anti-cooperative binding by SRP19 and SRP68/72 appears to arise from stabilization of distinct conformations in the stiff intervening RNA scaffold. Assembly of large RNPs is generally thought to involve either co-operative or energetically neutral interactions among components. By contrast, our findings emphasize that antagonistic interactions can play significant roles in assembly of multi-subunit RNPs.

Key words: anti-cooperativity, ribonucleoprotein assembly, signal recognition particle, structural communication.

INTRODUCTION

The SRP (signal recognition particle) is a ubiquitous phylogenetically conserved RNP (ribonucleoprotein) complex that mediates co-translational transport of secretory and membrane proteins [1–3]. The SRP binds simultaneously to a translating ribosome and to the hydrophobic N-terminal signal sequence of a nascent membrane-directed protein. The SRP then delivers the ribosome–nascent-chain complex to the membrane of the endoplasmic reticulum in eukaryotes or to the inner membrane in prokaryotes.

Although they share a common function, SRPs differ significantly in composition and mode of assembly across the major divisions of life, with eukaryotic SRPs being the most complex. The vertebrate SRP has an extended rod-shaped structure comprised of a ~300-nucleotide RNA and six proteins, and is organized into two domains, namely the *Alu* and the 'large' (or S) domain (Figure 1). The *Alu* domain contains proteins SRP9 and SRP14 and one-half of the SRP RNA. The large domain (hereafter referred to as LS) comprises proteins SRP19, SRP54, SRP68, SRP72 and the second half of the SRP RNA (LS RNA). Each of the two SRP domains can be assembled as separate complexes that retain their individual functions as characterized in the intact SRP [4,5].

Analysis of the interactions between the protein and RNA components of the mammalian SRP has proved to be a rich opportunity to understand the principles that govern assembly of complex multi-component RNPs. In the LS domain, SRP19 binds to the apices of RNA helices 6 and 8, thereby aligning the helices in parallel [6,7]. These SRP19-induced RNA conformational changes are an absolute prerequisite for subsequent RNA binding by SRP54 [8–10]. SRP54, the only universally conserved SRP protein, binds to conserved sequence elements in helix 8 [11,12] and performs several of the most critical functions of the SRP, including signal peptide recognition, interaction with the SRP receptor and GTP hydrolysis [1,2].

Interactions between mammalian SRP19 and SRP54 are remarkably elaborate. Formation of a stable SRP19–RNA complex is essential for high-affinity RNA binding by SRP54; however, simultaneous assembly of these two proteins with the SRP RNA leads to formation of a stable, but non-native, complex [10,13]. This order-of-interaction-driven misassembly suggests that structural biogenesis of the SRP may require a preferential order of interaction of SRP19 and SRP54 with the SRP RNA, as apparently occurs in the cell [14–16]. In the present study we discovered and analysed a second example of structural communication between protein components in the SRP, namely, RNA-mediated communication between SRP19 and SRP68/72.

SRP68 and SRP72 are the least characterized components in the SRP. These two proteins form a heterodimer [17,18] and bind at the three-way junction involving RNA helices 5, 6 and 8 [5,19,20]. A cryo-electron-microscopic study comparing free and ribosome-bound SRP structures showed that the SRP bends near its centre upon binding the nascent-chain–ribosome complex [5]. Electron density seen in this region was proposed to be the SRP68/72 heterodimer, which was suggested to act as an anchor between the large domain and a hinge in this region of the SRP RNA. Thus the SRP68/72 heterodimer may play a role in allowing movement of the two SRP domains to co-ordinate signal peptide recognition by the large domain with the elongation arrest activity of the *Alu* domain [5].

In the present study we addressed two important issues in assembly and function of the mammalian SRP. First, it is clear that the SRP68/72 heterodimer binds at the three-way junction in the SRP RNA [5,19,20]. However, the RNA binding properties of the individual proteins are poorly characterized. Secondly,

Abbreviations used: IPTG, isopropyl β-D-1-thiogalactopyranoside; LS RNA, large domain SRP RNA (positions 101–255); RNP, ribonucleoprotein; SRP, signal recognition particle; YT, yeast extract/tryptone.

[1] Correspondence may be addressed to either of these authors (email refried@email.unc.edu or weeks@unc.edu).

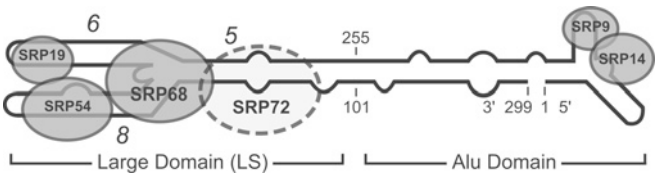

Figure 1 Architecture of the mammalian SRP

SRP proteins are shown as grey ovals. RNA is represented as a black line. The numbers 1, 101, 255, and 299 denote nucleotide positions and 5, 6, and 8 indicate major helices in the large domain (also identified as II, III and IV in an alternative convention [36]).

extensive evidence now supports the view that both the SRP19 and SRP68/72 components bind in the large domain and that both proteins have the ability to modulate the orientation of helices 5, 6 and 8. Whether these components interact co-operatively or antagonistically is unknown.

We find that SRP68 alone binds at the three-way junction linking helices 5, 6 and 8 on the opposite face of the SRP RNA relative to where SRP19 binds. In contrast, SRP72 has a strong, but apparently non-specific, ability to bind the SRP RNA. Thus SRP68 is responsible for most, or all, of the specific binding functions of the SRP68/72 heterodimer, whereas SRP72 increases the stability of the overall complex. Despite binding the opposite face of the RNA, both SRP68 alone and the SRP68/72 heterodimer stabilize an RNA conformation that is very similar to that induced by SRP19. Surprisingly, we find that mutual stabilization of a parallel orientation for helices 6 and 8 is anti-cooperative, such that prior binding by SRP19 decreases the affinity of SRP68/72 for the SRP RNA. Similarly, prior RNA binding by SRP68/72 diminishes the rate of binding by SRP19. SRP68/72 and SRP19 do not appear to contact each other directly in the SRP. Thus mutually anti-cooperative assembly may originate from stabilization of different conformations in the intervening RNA scaffold that oppose binding of the subsequent protein. Our findings suggest that competitive interactions are an important feature in the assembly of complex RNPs.

MATERIALS AND METHODS

Expression and purification of recombinant SRP proteins

C-terminal hexahistidine-tagged SRP68 and N-terminal hexahistidine-S-tagged SRP72 (both canine) were expressed from cDNAs cloned into plasmids pET42b and pET30a (Novagen) respectively. Expression of SRP68 was induced with 0.8 mM IPTG (isopropyl β-D-1-thiogalactopyranoside) for 5 h at 25 °C in *Escherichia coli* strain BL21(DE3)STAR (Invitrogen). SRP72 was expressed in BL21(DE3) (Novagen) pregrown to saturation at 37 °C in 2 × YT (yeast extract/tryptone) medium [1.6 % Bacto Tryptone (Difco), 0.5 % yeast extract (Difco) and 0.5 % NaCl] containing 1 % glucose. Cells were then diluted with 3 vol. of 2 × YT and incubated for 1 h at 37 °C, whereupon an equal volume of ice-cold medium containing 4 % (v/v) ethanol was added. Cells were incubated at 17 °C for 30 min and SRP72 expression was induced by addition of IPTG (to 1.0 mM) for 5 h at 17 °C. For both SRP68 and SRP72, cells were disrupted by sonication in 50 mM Tris/HCl, pH 7.5, 1.0 M LiCl, 5 mM 2-mercaptoethanol and 20 mM imidazole. A Branson Model #350 sonifier was used; the power setting was 40 % (140 W) with a flat-tipped probe and the time was 3 min total in 20 s bursts; the cells were suspended in 50 ml of the indicated buffer and sonication was carried out at 4 °C. After centrifugation for 1 h at 225 000 ***g***, the cleared lysate was applied to an Ni^{2+}-nitrilotriacetate–agarose column and was washed extensively using the same buffer. Proteins were eluted with 250 mM imidazole and dialysed into 25 mM Hepes/KOH, pH 7.5, 300 or 500 mM potassium acetate, 5 mM $MgCl_2$ and 5 mM 2-mercaptoethanol. SRP68 and SRP72 were estimated to be > 87 % and > 98 % pure as judged by integration of the purified protein bands resolved in a Coomassie Blue-stained denaturing SDS/polyacrylamide gel. The small amounts of additional peptides in the SRP68 preparations correspond to C-terminal fragments of 65 and 20 kDa. Pull-down assays using glutathione transferase-tagged SRP19 showed that, in the presence of the SRP LS RNA, neither of these fragments binds the RNA (results not shown). Thus the presence of these fragments has no affect on the conclusions made in this work. SRP19 was expressed and purified to homogeneity as described [6]. Protein concentrations were quantified using calculated absorption coefficients at 280 nm [21].

RNA–protein complex binding affinities

Internally ^{32}P-labelled full-length LS domain RNA (nts 101–255) was transcribed from plasmid Δ35 [22], purified by denaturing electrophoresis, and refolded by heating at 95 °C (1 min), snap-cooling on ice (1 min), incubating at 60 °C (10 min) in the presence of RNA refolding buffer (20 mM Hepes, pH 7.5, 300 or 500 mM potassium acetate, 5 mM $MgCl_2$ and 0.01 % Triton) and slow cooling (~ 40 min) to room temperature (25 °C) [10,23]. Final RNA concentrations were 0.1 nM. SRP68 and SRP72 protein binding reactions were performed at 25 °C in RNA refolding buffer ± 0.1 mg/ml BSA; reactions containing SRP19 were supplemented with 0.2 vol. of 50 mM sodium phosphate buffer, pH 8.0, 300 mM NaCl and 0.5 mg/ml BSA. For measurements of SRP68/72 binding to the preformed SRP19–RNA complex (at 500 mM potassium acetate; shown in Figure 6A below), SRP19 was added to the RNA 30 min prior to SRP68/72 addition. Protein–RNA complexes were rapidly partitioned from free RNA by filtering through nitrocellulose (top membrane, from Schleicher and Schuell) and HyBond™ N+ (bottom membrane, from Amersham), using a dot-blot apparatus (Schleicher and Schuell) and quantified by phosphorimaging. Equilibrium dissociation constants (K_d) were obtained by using the following equation:

$$\text{Fraction of RNA bound} = A \cdot K_d/(K_d + [\text{protein}])$$

where A is the maximum fraction of RNA–protein complex retained on the nitrocellulose filter.

Hydroxyl-radical footprinting

5′-^{32}P-labelled LS RNA (50 nM) was incubated with the appropriate SRP protein(s) in RNA refolding buffer. For low-ionic-strength (300 mM potassium acetate) experiments, the final concentration of each SRP protein was 100 nM. For 500 mM potassium acetate experiments, SRP68 (800 nM), SRP72 (800 nM) or SRP68/72 (200, 400 and 800 nM) were used. Hydroxyl-radical cleavage (25 °C, 1 h) was initiated by adding freshly prepared solutions (2 μl each) of 30 mM $[Fe(II)(NH_4)_2]SO_4$/45 mM EDTA, 50 mM dithiothreitol and 50 mM sodium ascorbate to a 20 μl reaction volume. Reactions were quenched by adding 2 μl of 2 M thiourea, 2 μl of 0.5 M EDTA and 20 μg of proteinase K (37 °C, 30 min). RNA fragments were resolved on denaturing 8–12%-(w/v)-polyacrylamide sequencing gels and quantified by phosphorimaging. Pymol (www.pymol.org) was used to visualize

protein interaction sites in the context of an SRP19–RNA crystal structure [7].

SRP19 assembly kinetics

SRP19 was labelled with an Alexa 488 fluorophore at unique cysteine residues at positions 31 or 72 as described in [13]. Experiments were performed in RNA refolding buffer containing 500 mM potassium acetate, supplemented with 0.2 vol. of 50 mM sodium phosphate, pH 8.0, and 300 mM NaCl at 25 °C. Assembly of SRP19 with the free RNA or with the SRP68/72–RNA complex was initiated by adding 100 μl of refolded LS RNA (100 nM final concn.) or preformed SRP68/72–RNA complex (100 nM final concn.) to 400 μl of Alexa 488-labelled SRP19 (25 nM final concn.). Fluorescence emission from the Alexa 488 fluorophore was monitored as a function of time using a Varian/Cary Eclipse spectrofluorimeter and was fitted to a second-order rate equation. For SRP 19 tagged at residue 72, fluorescence data were fitted to:

$$\text{Fluorescence} = A\{[\exp(kc_1t) - \exp(kc_2t)](c_1c_2)/[c_1\exp(kc_1t) - c_2\exp(kc_2t)]\} + b$$

where k is the second-order rate constant, c_1 and c_2 are the initial concentrations of SRP19 and either the free RNA or the SRP68/72–RNA complex, A is the amplitude of the fluorescence change and b is the initial fluorescence of the preformed SRP68/72–RNA complex. For SRP19 tagged at position 31, A minus the right side of the equation was used.

RESULTS

Ionic-strength-dependent RNA binding by SRP68 and SRP72

Our goal in the present study was to analyse potential inter-dependent interactions between the SRP19, SRP68 and SRP72 proteins as they assemble with the SRP RNA. In prior work on the SRP, different ionic conditions have been used for studies in which SRP has been assembled in whole or in part. Importantly, in their pioneering investigations, Walter and Blobel [17] showed that the SRP could be reconstituted under a variety of ionic conditions (150–500 mM potassium acetate or 4–20 mM $MgCl_2$) without affecting function. This finding probably accounts for the apparent lack of a consensus regarding optimal conditions for *in vitro* assembly experiments, although more recent studies have mostly employed higher ion concentrations (300–500 mM potassium acetate; for recent examples, see [20,24–30]). Despite the seemingly small effect of these differing assembly conditions, two previous studies reached different conclusions regarding the RNA binding properties of the individual SRP68 and SRP72 proteins [28,31]. In 500 mM potassium acetate, SRP72 did not form a detectable complex with the SRP RNA [31], whereas, at lower ionic strengths, C-terminal peptide fragments of SRP72 appeared to bind the RNA [28]. Therefore, in exploratory experiments, we re-examined the *in vitro* RNA binding properties of recombinant SRP68 and SRP72 in equilibrium-filter-partitioning experiments [6] at both 300 mM and 500 mM potassium acetate using the LS RNA (Figure 1).

At 300 mM potassium acetate, SRP68 had a low affinity for the RNA with a measured K_d of $\geqslant 250$ nM (Figure 2A). By contrast, SRP72 bound relatively tightly to the RNA, characterized by a dissociation constant (K_d) of 23 nM. SRP68 and SRP72 together bound the RNA with an affinity ($K_d = 8$ nM) that was about 3-fold higher than that of SRP72 alone (compare SRP68/72 and SRP72 binding experiments in Figure 2A).

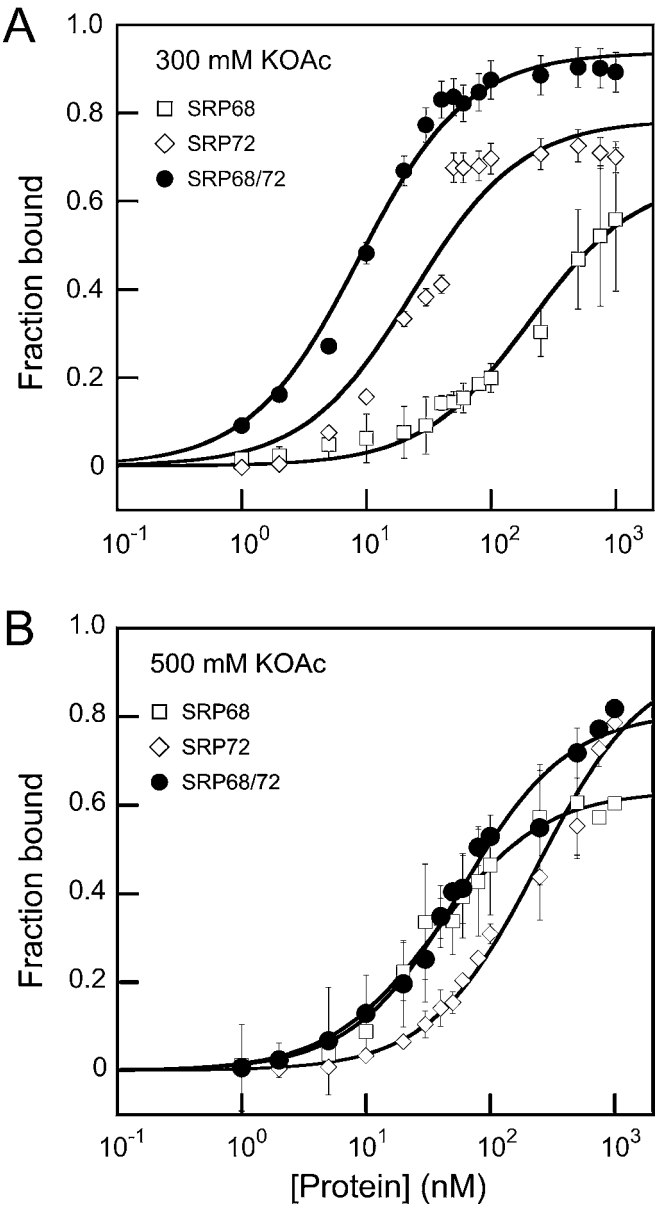

Figure 2 RNA binding by SRP68 and SRP72

Fraction of bound RNA as a function of SRP protein concentration was determined by filter partitioning. Equilibrium dissociation constants (K_d) are: at 300 mM potassium acetate (KOAc): SRP68 $\geqslant$ 250 nM, SRP72 = 23 nM, SRP68/72 = 8 nM; at 500 mM potassium acetate: SRP68 = 36 nM, SRP72 $\geqslant$ 250 nM, SRP68/72 = 57 nM. Error bars indicate the S.D. for two independent experiments.

The RNA-binding properties for both SRP68 and SRP72 were different at 500 mM potassium acetate (Figure 2B). SRP68 bound to the RNA with significantly higher affinity ($K_d = 36$ nM) than at 300 mM potassium acetate, whereas SRP72 binding was significantly weakened ($K_d \geqslant 250$ nM). When both proteins were present, the binding affinity ($K_d = 57$ nM) was similar to that measured for SRP68 alone (compare SRP68/72 and SRP68 experiments in Figure 2B). Because the binding affinities of SRP68 and SRP68/72 were similar, SRP72 either makes no contribution to binding at the higher (500 mM) potassium acetate concentration or does not form a complex with SRP68 under these conditions.

These results indicate that the RNA-binding properties of both SRP68 and SRP72 are modulated by the solution ionic

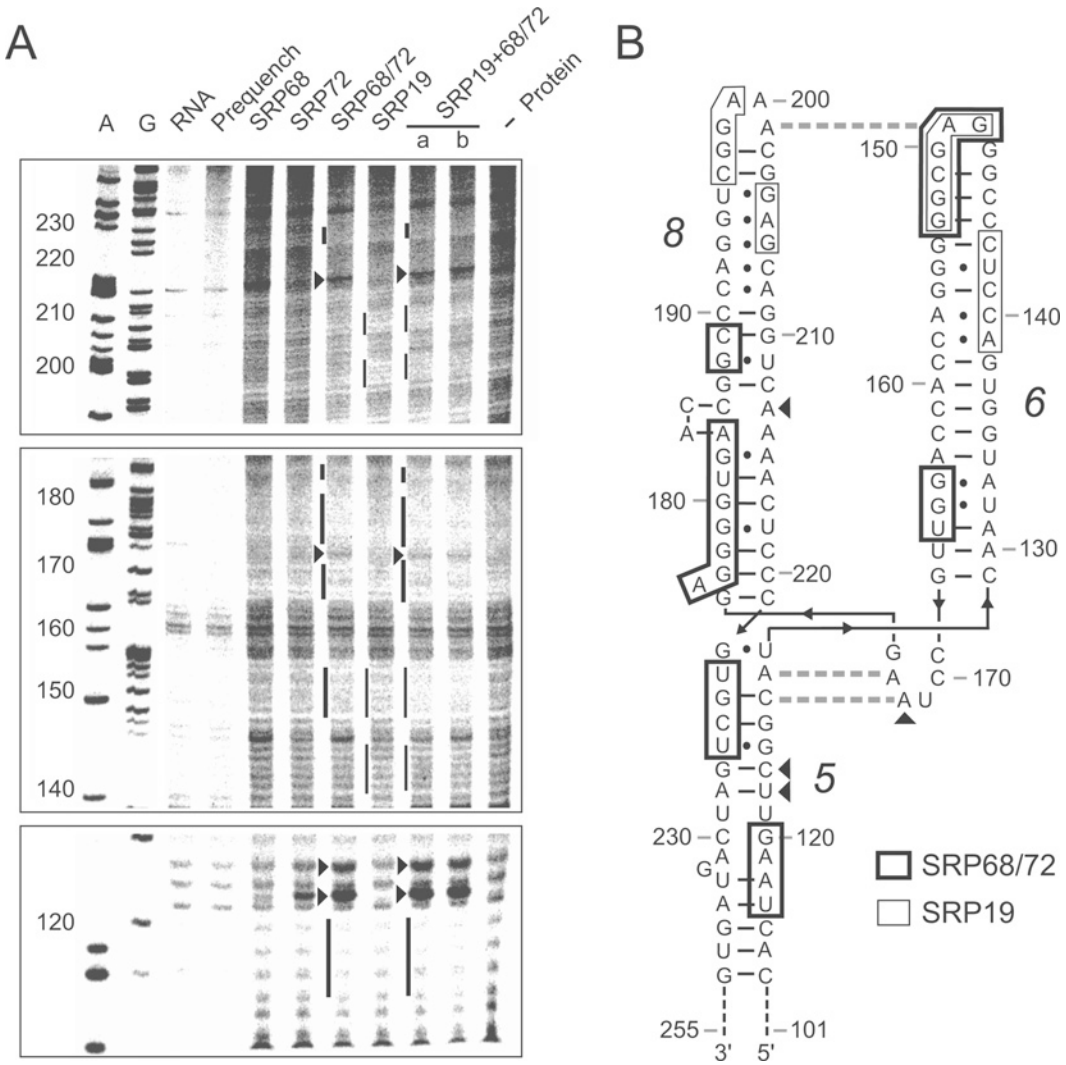

Figure 3 SRP68/72 and SRP19 interaction sites on the SRP RNA at 300 mM potassium acetate

(**A**) Hydroxyl-radical footprinting visualized by denaturing gel electrophoresis. Nucleotides that are specifically protected from hydroxyl-radical cleavage upon binding by SRP68/72 and SRP19 are emphasized with thick and thin black lines respectively. Nucleotides with enhanced reactivity upon SRP68/72 binding are shown by the closed arrowheads (►). 'a' and 'b' in the SRP19 + SRP68/72 lane differ by the order in which proteins were added to the RNA. Prequench indicates RNA that was incubated with the thiourea quenching agent prior to initiation of the cleavage reaction. For clarity, the central region of this gel image has been omitted. (**B**) Superimposition of hydroxyl-radical protection on the LS RNA secondary structure. Nucleotides protected upon binding by SRP68/72 and SRP19 are enclosed in thick and thin lined boxes respectively; closed arrowheads indicate enhanced cleavage upon SRP68/72 binding. The RNA sequence spanned the entire LS domain (positions 101–255); for clarity, only positions showing specific protection from hydroxyl-radical-induced cleavage are shown.

environment, but in opposite ways: higher ionic strength favours RNA binding by SRP68, whereas lower ionic strength favours binding by SRP72. In addition, RNA binding by SRP68 and SRP72 is moderately co-operative at 300 mM potassium acetate, but this enhanced binding is not observed at 500 mM. These experiments reconcile the previous divergent results regarding SRP68/SRP72 binding by showing that SRP72 has low affinity for the SRP RNA at 500 mM potassium acetate, a concentration that is widely used in SRP assembly and reconstitution experiments [17,24,25,27,31,32], but that affinity increases significantly at lower univalent-ion concentrations. In the study reported here, these ion-concentration experiments simply provide a useful tool for dissecting the distinct binding properties of SRP68 and SRP72 and their role in assembly of the SRP. At 500 mM potassium acetate, binding by SRP68 can be studied without significant contributions of binding by SRP72.

SRP19 and SRP68 bind on opposite faces of the SRP RNA

We used hydroxyl-radical footprinting experiments to identify interaction sites between SRP68 and SRP72 and the LS RNA. The Fe(II)–EDTA-mediated hydroxyl-radical reagent reacts with solvent-accessible sites and induces cleavage in the RNA backbone at positions that are not occluded by either RNA–RNA or RNA–protein interactions [33,34].

We first carried out hydroxyl-radical cleavage experiments at 300 mM potassium acetate using diagnostic combinations of SRP19, SRP68 and SRP72 (each at 100 nM concentration; Figure 3A). Protection specific to an SRP protein was identified by comparing RNA cleavages in the presence of the protein relative to those obtained in its absence. Alone, neither SRP68 nor SRP72 yielded significant protection from hydroxyl-radical-induced cleavage (compare SRP68 and SRP72 lanes with the

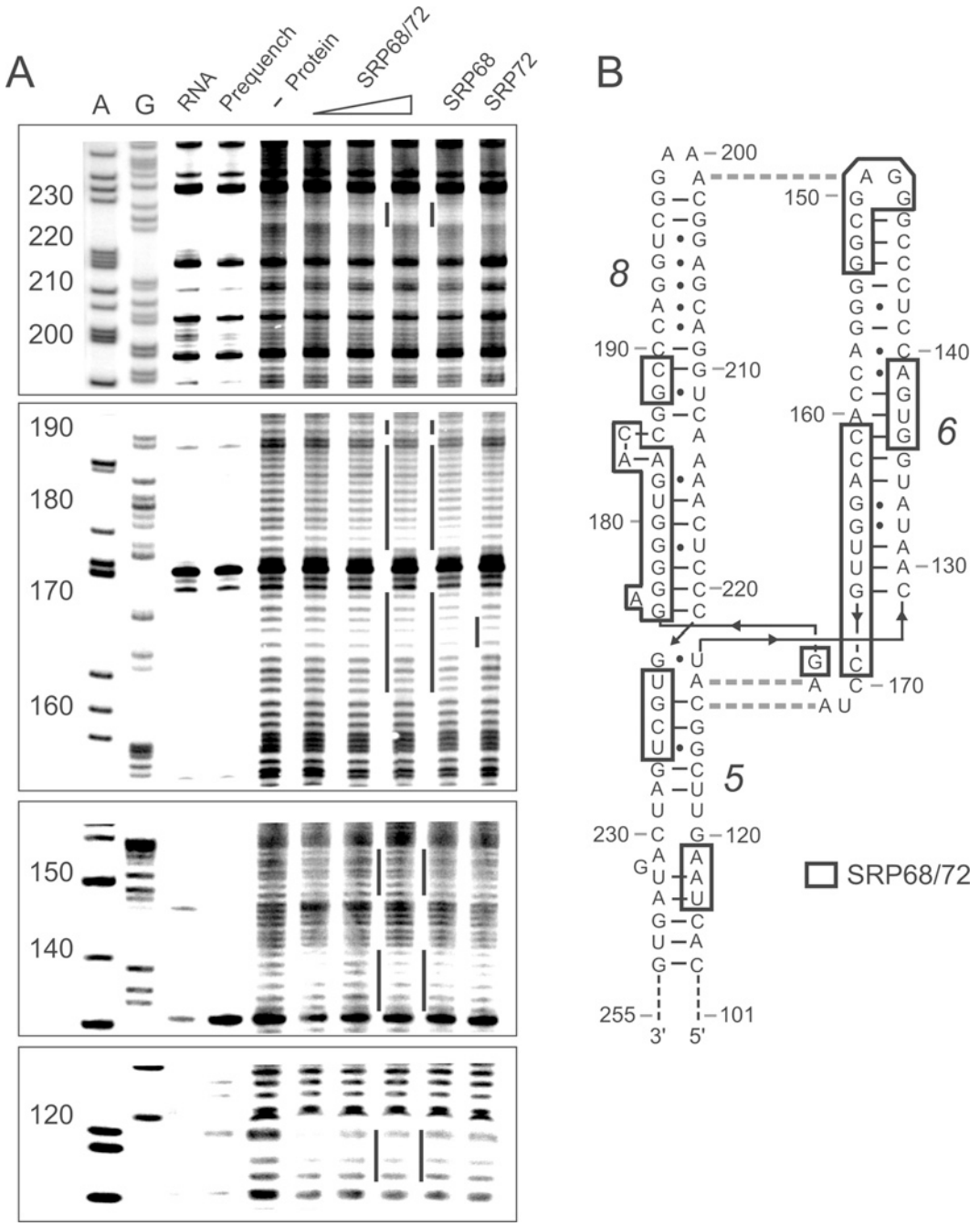

Figure 4 SRP68 interaction sites on the SRP RNA at 500 mM potassium acetate

(**A**) Nucleotides that are specifically protected from hydroxyl-radical cleavage upon protein binding are emphasized by black lines. (**B**) Superposition of SRP68-induced protection from hydroxyl-radical cleavage (boxes) on the secondary structure of the LS RNA.

'– Protein' lane in Figure 3A). Protection in the presence of SRP68 was not expected, because SRP68 does not form a stable complex with the RNA either under these conditions or at much higher concentrations (Figure 2A). SRP72 binding to the LS RNA is saturating under these conditions (Figure 2A), and the absence of a detectable protection pattern suggests that SRP72 may not interact at a single well-defined site in the RNA.

In contrast, addition of both SRP68 and SRP72 protected a large number of nucleotides from hydroxyl-radical-mediated cleavage (compare SRP68/72 lane with the '– Protein' lane in Figure 3A; protected nucleotides are indicated by thick vertical black lines). Protected positions span each of the helices 5, 6 and 8 in the LS RNA (boxes with thick lines; Figure 3B). In addition to these protected regions, four nucleotides consistently showed enhanced reactivity upon binding by SRP68/72, namely U^{122}, C^{123}, A^{172} and A^{213} [closed arrowheads (◄) in Figure 3].

We also identified the nucleotides that became protected from hydroxyl-radical-mediated cleavage in the presence of SRP19. These nucleotides reside mainly at the apical loops of helices 6 and 8 in the RNA (thin vertical lines in SRP19 lane in Figure 3A and thin boxes in Figure 3B). This protection pattern corresponds well with the findings from previous footprinting experiments [6]

and with high-resolution structures of the SRP19–RNA complex [7,35]. When footprinting experiments were performed in the presence of both SRP19 and SRP68/72, the protected nucleotides were consistent with a simple combination of those for the individual protein components (see SRP19+SRP68/72 lanes in Figure 3A).

We next used hydroxyl-radical footprinting to evaluate RNA binding by SRP68 and SRP72 at 500 mM potassium acetate. At this ionic strength, SRP68 has significantly higher affinity for the RNA, whereas SRP72 binds 10-fold more weakly as compared with the 300 mM potassium acetate condition (Figure 2B). SRP72 alone yielded almost no significant footprint on the RNA, except at nucleotides 165–168 (Figure 4A). In contrast, SRP68 by itself then produced a clear RNA footprint that was very similar to that observed for the SRP68/72–RNA ternary complex at 300 mM potassium acetate (see the SRP68 lane in Figure 4A, protected nucleotides are illustrated by vertical black lines). Finally, addition of both proteins yielded a footprint that was identical with that produced by SRP68 alone (compare SRP68 and SRP68/72 lanes; Figure 4A). The nucleotides protected upon SRP68 binding are superimposed on the LS RNA secondary structure in Figure 4(B).

These equilibrium binding and hydroxyl radical footprinting experiments support two self-consistent conclusions regarding SRP68 and SRP72 interactions with the LS RNA. First, neither SRP68 nor SRP72 produced a specific footprint at 300 mM potassium acetate, whereas the two proteins together yielded a well-defined footprint on the RNA (Figure 3A). Thus, as judged by both equilibrium binding measurements (Figure 2A) and footprinting, specific RNA binding by SRP68 and SRP72 under these conditions involves mutually reinforcing interactions between these two proteins. Secondly, the experiments performed at 500 mM potassium acetate indicate that most of the direct interactions between SRP68/72 and the RNA are mediated by SRP68 alone.

We visualized nucleotides protected by SRP68/72 and SRP19 in the context of a three-dimensional structure of the LS RNA in its SRP19-bound conformation [7] (Figure 5; SRP68/72 and SRP19 footprints are shown in grey). The primary interaction sites for SRP68/72 lie at the three-helix junction and on the opposite face of the RNA relative to where SRP19 binds. This interaction site is also consistent with recent footprinting experiments using dimethyl sulfate carried out under comparable ionic-strength conditions [20]. Overall, RNA positions affected by SRP68/72 binding are quite broad and extend from the tip of helix 6 to the middle of helix 5 (Figure 5).

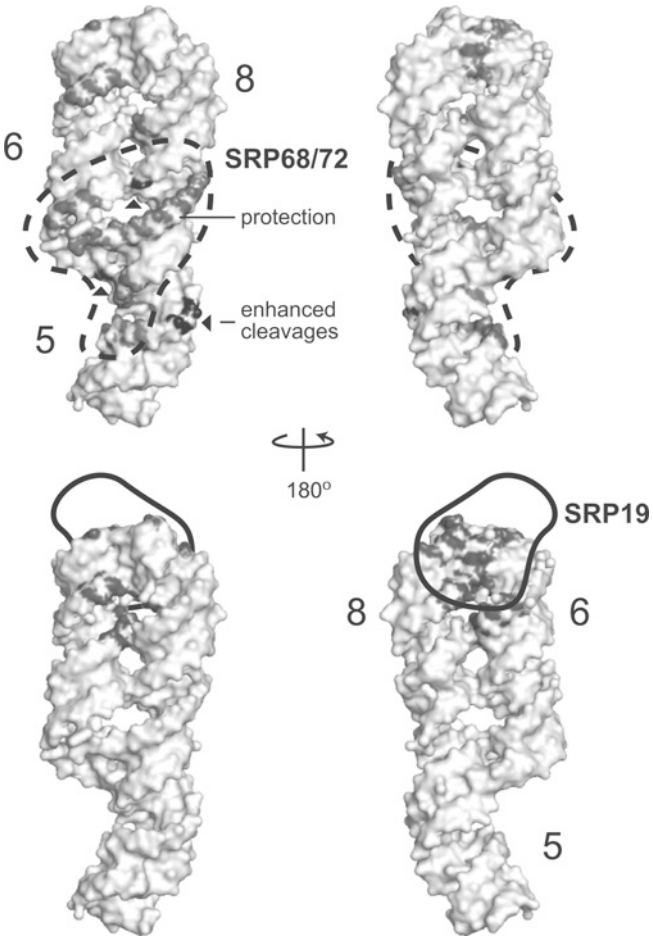

Figure 5 Visualization of the SRP68/72 and SRP19 interaction sites on a three-dimensional model based on the binary SRP19–RNA complex [7]

The solid outline in the lower half represents the space occupied by SRP19. RNA ribose groups protected from hydroxyl-radical cleavage in the presence of SRP68/72 and SRP19 are shown in grey. Regions showing enhanced reactivity upon SRP68/72 binding are identified by two closed triangles.

SRP19 and SRP68/72 bind the SRP RNA anti-co-operatively

Although the primary interaction sites for SRP19 and SRP68/72 lie on opposite faces of the LS RNA, both contact the same two RNA helices and also protect similar structures at the apex of helix 6 (Figures 3 and 5; see also [5,9,12,18,19]). We therefore sought to assess the extent to which SRP19 and SRP68/72 interact cooperatively with the RNA. We compared the affinity of SRP68/72 binding to the free RNA versus that to the preformed SRP19–RNA complex using a filter partitioning assay. The 500 mM potassium acetate condition was chosen to minimize the effect of non-specific RNA binding by SRP72 (see Figure 2). This experiment took advantage of the fact that SRP19 binds to the LS RNA ~75-fold more tightly than does SRP68/72 under this ionic-strength condition. When the concentration of SRP19 is subsaturating, binding by SRP68/72 can be measured as the increase in nitrocellulose-filter retention of the SRP68/72–SRP19–RNA complex relative to that of the SRP19–RNA complex alone. We report the results of these binding experiments in two ways. The main panel in Figure 6(A) shows the increase in absolute nitrocellulose filter retention for binding by SRP68/72 to the free RNA (closed symbols) and for binding to pre-formed SRP19-RNA complexes (open symbols). To illustrate the net effect of pre-binding by SRP19 more clearly, we also show the same data in which all changes in filter binding efficiency are normalized to the same scale spanning 0–1.0 (inset to Figure 6A).

In this series of experiments, the SRP68/72–RNA complex had a K_d of 28 nM (closed symbols, Figure 6A). When the RNA was preincubated with 0.38, 0.50 and 0.75 nM SRP19, the apparent K_d for SRP68/72 increased to 44, 82 and 95 nM respectively (open symbols, Figure 6A). A plot of the apparent K_d for SRP68/72 binding as a function of the fraction of RNA bound by SRP19 yielded a linear relationship (Figure 6B). When extrapolated to saturating RNA binding by SRP19, complete prior binding by SRP19 would yield a K_d for SRP68/72 of ~160 nM, which represents a 5-fold inhibition of SRP68/72 binding to the LS RNA by SRP19.

We next monitored the reciprocal effect of prior RNA binding by SRP68/72 on the ability of SRP19 to bind the LS RNA, using kinetic measurements (Figure 7). In these experiments,

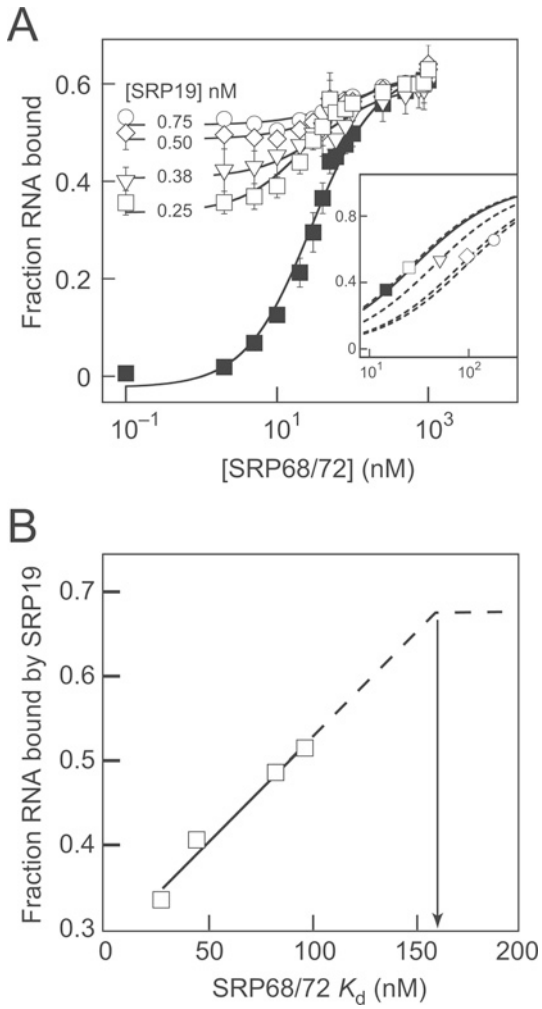

Figure 6 Anti-co-operative RNA binding by SRP68/72 and SRP19

(**A**) RNA binding affinity of SRP68/72 for the free LS RNA (■; $K_d = 28$ nM) and for pre-formed SRP19–LS RNA complexes (open symbols). The inset shows the same data with transition amplitudes normalized to a scale from 0 to 1. Each curve reflects the average results from three sets of independent experiments. (**B**) Relationship between the fraction RNA bound by SRP19 and the K_d for SRP68/72 binding to the LS RNA complexes. The arrow shows extrapolation of the K_d for SRP68/72–RNA complexes to saturating concentrations of SRP19.

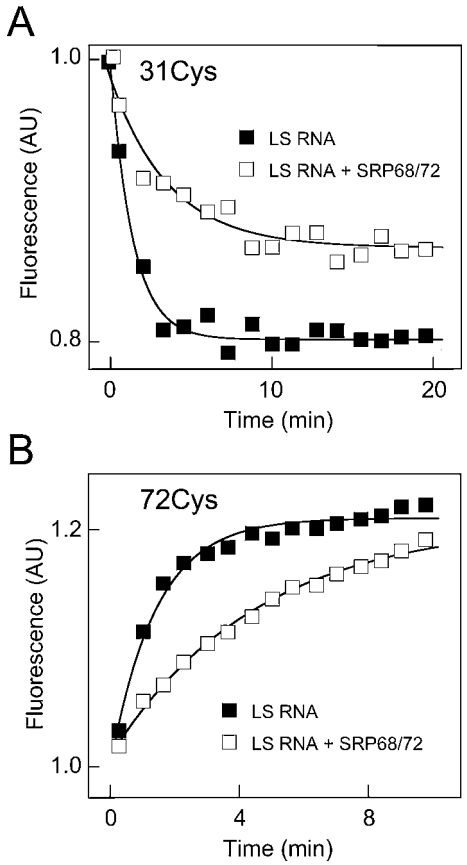

Figure 7 Inhibition of SRP19–RNA complex formation by prior binding by SRP68/72

(**A**) Association of SRP19 with the LS RNA monitored by the change in fluorescence emission for an Alexa 488 fluorophore tethered to SRP19 at residue 31 [13]. SRP19 binding to the free RNA versus to a preformed SRP68/72–RNA complex are shown with closed and open symbols respectively. (**B**) Association of SRP19 with the LS RNA monitored by the change in fluorescence emission for an Alexa 488 fluorophore tethered to SRP19 at residue 72. Assembly rate constants were calculated by fitting results to a complete second-order kinetic rate equation (continuous lines). Abbreviation: AU, arbitrary units.

an Alexa 488 fluorophore was tethered either at position 31 or 72 in SRP19 via unique cysteine residues (termed the '31Cys' and '72Cys' variants), as previously described [13]. These Alexa 488-tethered SRP19 derivatives have an RNA binding behaviour that is indistinguishable from that of the native protein [13]. When the Alexa 488-labelled SRP19 proteins bind to the LS RNA, the environment around the tethered fluorophore changes to yield either a decrease (position 31) or an increase (position 72) in fluorescence emission. We therefore monitored the change in fluorescence over time during the assembly of SRP19 with the LS RNA. SRP19 tagged at position 31 bound to the free RNA with a second-order rate constant $8.4 \times 10^6\ M^{-1} \cdot min^{-1}$ (closed symbols, Figure 7A), which is within 3-fold of our previously reported value measured under the lower, 300 mM, salt condition [13]. When the analogous experiment was performed using a preformed SRP68/72–RNA complex, the SRP19 binding rate decreased by almost 3-fold to $3.1 \times 10^6\ M^{-1} \cdot min^{-1}$ (open symbols, Figure 7A). We then performed similar experiments using SRP19 carrying a fluorescent label at position 72. The 72Cys SRP19 bound the free LS RNA with a second-order rate constant of $7.9 \times 10^6\ M^{-1} \cdot min^{-1}$, a value that matches the previously reported rate (closed symbols, Figure 7B). Pre-binding by SRP68/72 decreased the second-order rate constant by more than 3-fold to $2.2 \times 10^6\ M^{-1} \cdot min^{-1}$ (open symbols, Figure 7B). These experiments emphasize that prior RNA binding by SRP68/72 inhibits binding by SRP19.

Thus, as judged by both equilibrium binding (Figure 6) and kinetic association experiments (Figure 7), RNA binding by SRP19 and SRP68/72 are modestly anti-cooperative. Prior binding by either protein decreases either the affinity or rate of subsequent RNA binding by the second protein component.

DISCUSSION

In the present study we addressed two previously unexplored questions regarding assembly of the mammalian SRP. First, we characterized the RNA-binding properties of the individual SRP68 and SRP72 proteins and found that SRP68 is primarily responsible for forming specific interactions with the SRP RNA. Secondly, although both SRP19 and SRP68/72 modulate the orientation of SRP RNA helices 5, 6 and 8, we have now shown that this modulation is anti-co-operative.

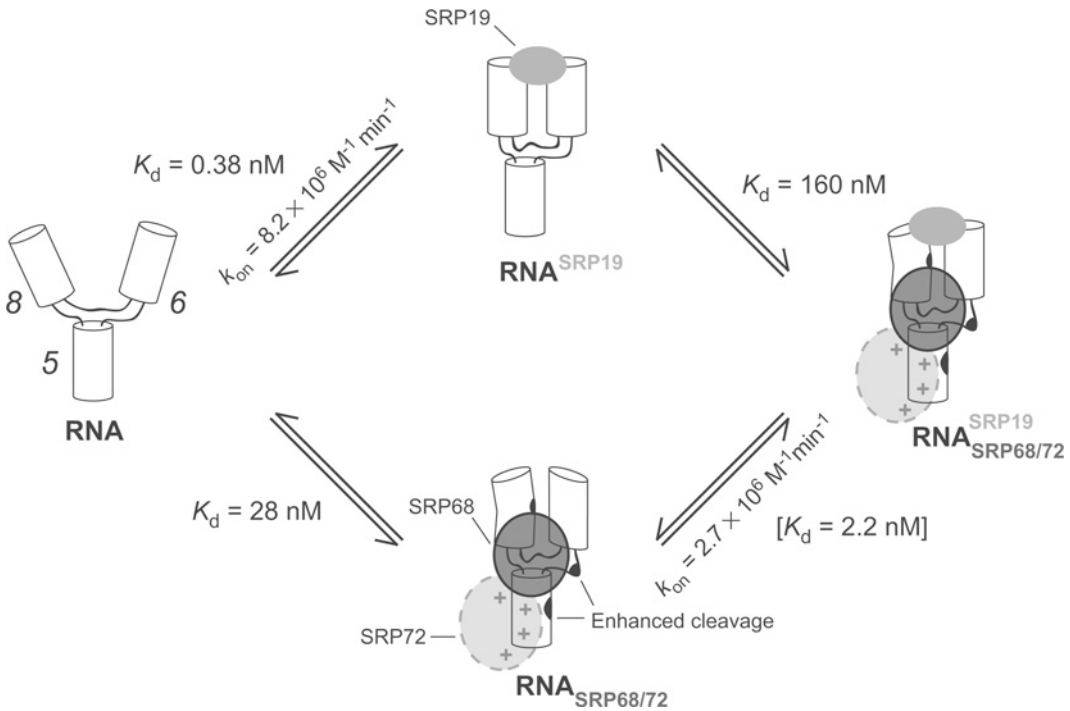

Figure 8 Model for anti-cooperative assembly of SRP19 and SRP68/72 with the SRP RNA

SRP19 and SRP68/72 are shown as grey ovals; '+' signs emphasize electrostatic binding by SRP72. Helices 6 and 8 are drawn to show that SRP19 and SRP68/72 stabilize distinct RNA conformations; regions that show enhanced cleavage in the presence of SRP68 are in solid black. The K_d value in square brackets was calculated from other values. The rate constants shown for SRP19 assembly are the average of those measured for SRP19 labelled at residues 31 and 72.

Non-specific binding by SRP72 enhances specific SRP68–RNA interactions

At 500 mM potassium acetate, SRP68 binds with 36 nM affinity to the RNA and, by itself, can account for the entire set of interactions between the SRP68/72 heterodimer and the LS RNA that are protected from hydroxyl-radical footprinting (Figures 3 and 4). Conversely, despite relatively tight binding affinity at 300 mM potassium acetate ($K_d = 23$ nM), SRP72 does not protect the LS RNA from hydroxyl-radical cleavage (Figure 3). These findings suggest binding by SRP72 to the RNA is mediated by relatively strong, but non-specific, electrostatic interactions.

Together, these results are consistent with a general model for the SRP68/72 heterodimer in which SRP68 is the protein component that forms structurally specific interactions at the RNA junction formed by helices 5, 6 and 8. SRP72 does enhance binding by SRP68, although this effect is strongly dependent on the monovalent ion concentration. We postulate that SRP72 stabilizes the ribonucleoprotein complex, primarily via non-specific electrostatic interactions (bottom of the scheme in Figure 8).

Anti-co-operative interactions in SRP assembly

SRP19 and the SRP68/72 heterodimer both bind to helices 6 and 8 in the SRP RNA, but on opposite faces and at opposite ends. SRP19 binds at the apical loops of helices 6 and 8, whereas SRP68/72 binds at the three-way helical junction formed by helices 5, 6 and 8 (Figure 5). The free LS RNA has a flexible structure in which most of the individual base-pairs are formed, but helices 6 and 8 do not stably interact with each other [6]. Binding by SRP19 induces a conformational change in the RNA and juxtaposes and aligns helices 6 and 8 in parallel (Figure 5) [6,7]. Binding by SRP68 also causes a conformational change in the RNA extending to the tip of helix 6 (Figures 4 and 5 and [16,19]). SRP68 and SRP19 thus both appear to induce an overall conformation in the RNA such that helices 6 and 8 are roughly parallel (centre two structures in Figure 8).

Despite stabilizing globally similar conformations for helices 6 and 8, SRP19 and SRP68/72 bind anti-co-operatively to the RNA. Experimentally, prior binding by SRP19 reduces the affinity of SRP68/72 for the RNA by 5-fold (Figure 6). Similarly, prior binding by SRP68/72 decreases the rate of RNA binding by SRP19 by 3-fold (Figure 7). These experiments emphasize that neither binding by SRP19 nor by SRP68/72 stabilizes an RNA conformation that optimally facilitates binding by the second component (emphasized by distinct helix conformations; Figure 8).

This model is further corroborated by hydroxyl-radical-footprinting experiments performed at 300 mM potassium acetate (Figure 3). In the presence of both SRP68 and SRP72, three regions in the RNA show enhanced hydroxyl-radical cleavage (solid black regions in Figure 8). Independent work has also shown that some of these regions exhibit enhanced reactivity towards dimethyl sulfate in the presence of SRP68/72 [20]. These observations suggest that, upon binding by SRP68/72, the RNA acquires a conformation in which these nucleotides are more highly exposed to solvent than in the free RNA. In contrast, these regions are not hyper-reactive in the SRP19–RNA binary complex, indicating that SRP68/72 and SRP19 induce distinct conformations in the LS RNA.

Assembly of large RNPs generally has been thought to involve either cooperative or energetically neutral interactions among components such that early assembly events tend to facilitate protein binding in subsequent steps. Models that imply cooperative interaction among components have been proposed for the

SRP [20]. In contrast with this view, direct measurements of the interactions between proteins show that binding by SRP19 and SRP68/72 is anti-co-operative. The extent of this anti-cooperativity, amounting to 0.7–1.0 kcal/mol (1 kcal = 4.184 kJ), could have important implications for SRP assembly *in vivo*. Binding by SRP19 to the SRP RNA is a multistep process which is sufficiently slow that the simultaneous presence of SRP54 prevents formation of the native SRP19–SRP RNA complex [10,13]. Cells appear to avoid this interference by assembling SRP19 with the SRP RNA in the nucleus while confining SRP54 to the cytoplasm [10,15]. Since binding by SRP68/72 further slows SRP19 binding to the SRP RNA, the necessity for compartmentalized assembly would be even more important to prevent misassembly of the complete SRP large domain. We propose that anti-co-operative assembly by SRP19 and SRP68/72 is communicated, in part, by the stiff RNA elements that separate the binding sites for these proteins (Figure 8). Given the long-distance rigidity of RNA helices and the complexity of many RNP complexes, it is likely that other examples of anti-co-operative RNP assembly remain to be discovered.

We thank Professor Dr Bernhard Dobberstein [ZMBH (Center for Molecular Biology Heidelberg), University of Heidelberg, Heidelberg, Germany] for cDNA clones of SRP68 and SRP72 and Professor Dr Dirk Görlich (ZMBH, University of Heidelberg, Heidelberg, Germany) for helpful discussions. Supported by grants from the National Institutes of Health (GM065491 to K. M. W.) and the National Science Foundation (MCB-9817104 to H. M. F.).

REFERENCES

1 Keenan, R. J., Freymann, D. M., Stroud, R. M. and Walter, P. (2001) The signal recognition particle. Annu. Rev. Biochem. **70**, 755–775
2 Doudna, J. A. and Batey, R. T. (2004) Structural insights into the signal recognition particle. Annu. Rev. Biochem. **73**, 539–557
3 Pool, M. R. (2005) Signal recognition particles in chloroplasts, bacteria, yeast and mammals. Mol. Membr. Biol. **22**, 3–15
4 Siegel, V. and Walter, P. (1988) Each of the activities of signal recognition particle (SRP) is contained within a distinct domain: analysis of biochemical mutants of SRP. Cell **52**, 39–49
5 Halic, M., Becker, T., Pool, M. R., Spahn, C. M. T., Grassucci, R. A., Frank, J. and Beckmann, R. (2004) Structure of the signal recognition particle interacting with the elongation-arrested ribosome. Nature **427**, 808–814
6 Rose, M. A. and Weeks, K. M. (2001) Visualizing induced fit in early assembly of the human signal recognition particle. Nat. Struct. Biol. **8**, 515–520
7 Oubridge, C., Kuglstatter, A., Jovine, L. and Nagai, K. (2002) Crystal structure of SRP19 in complex with the S domain of SRP RNA and its implication for the assembly of the signal recognition particle. Mol. Cell **9**, 1251–1261
8 Romisch, K., Webb, J., Herz, J., Prehn, S., Frank, R., Vingron, M. and Dobberstein, B. (1989) Homology of 54K protein of signal-recognition particle, docking protein and two *E. coli* proteins with putative GTP-binding domains. Nature **340**, 478–482
9 Gowda, K., Chittenden, K. and Zwieb, C. (1997) Binding site of the M-domain of human protein SRP54 determined by systematic site-directed mutagenesis of signal recognition particle RNA. Nucleic Acids Res. **25**, 388–394
10 Maity, T. S., Leonard, C. W., Rose, M. A., Fried, H. M. and Weeks, K. M. (2006) Compartmentalization directs assembly of the signal recognition particle. Biochemistry **45**, 14955–14964
11 Batey, R. T., Rambo, R. P., Lucast, L., Rha, B. and Doudna, J. A. (2000) Crystal structure of the ribonucleoprotein core of the signal recognition particle. Science **287**, 1232–1239
12 Kuglstatter, A., Oubridge, C. and Nagai, K. (2002) Induced structural changes of 7S L RNA during the assembly of human signal recognition particle. Nat. Struct. Biol. **9**, 740–744
13 Maity, T. S. and Weeks, K. M. (2007) A three-fold RNA–protein interface in the signal recognition particle gates native complex assembly. J. Mol. Biol. **369**, 512–524
14 Jacobson, M. R. and Pederson, T. (1998) Localization of signal recognition particle RNA in the nucleolus of mammalian cells. Proc. Natl. Acad. Sci. U.S.A. **95**, 7981–7986
15 Politz, J. C., Yarovoi, S., Kilroy, S. M., Gowda, K., Zwieb, C. and Pederson, T. (2000) Signal recognition particle components in the nucleolus. Proc. Natl. Acad. Sci. U.S.A. **97**, 55–60
16 Alavian, C. N., Politz, J. C. R., Lewandowski, L. B., Powers, C. M. and Pederson, T. (2004) Nuclear export of signal recognition particle RNA in mammalian cells. Biochem. Biophys. Res. Commun. **313**, 351–355
17 Walter, P. and Blobel, G. (1983) Disassembly and reconstitution of signal recognition particle. Cell **34**, 525–533
18 Scoulica, E., Krause, E., Meese, K. and Dobberstein, B. (1987) Disassembly and domain structure of the proteins in the signal-recognition particle. Eur. J. Biochem. **163**, 519–528
19 Siegel, V. and Walter, P. (1988) Binding sites of the 19-kDa and 68/72-kDa signal recognition particle (SRP) proteins on SRP RNA as determined by protein-RNA "footprinting". Proc. Natl. Acad. Sci. U.S.A. **85**, 1801–1805
20 Menichelli, E., Isel, C., Oubridge, C. and Nagai, K. (2007) Protein-induced conformational changes of RNA during the assembly of human signal recognition particle. J. Mol. Biol. **367**, 187–203
21 Gill, S. C. and von Hippel, P. H. (1989) Calculation of protein extinction coefficients from amino acid sequence data. Anal. Biochem. **182**, 319–326
22 Zwieb, C. (1991) Interaction of protein SRP19 with signal recognition particle RNA lacking individual RNA-helices. Nucleic Acids Res. **19**, 2955–2960
23 Gowda, K. and Zwieb, C. (1997) Determinants of a protein-induced RNA switch in the large domain of signal recogntition particle identified by systematic-site directed mutagenesis. Nucleic Acids Res. **25**, 2835–2840
24 Janiak, F., Walter, P. and Johnson, A. E. (1992) Fluorescence-detected assembly of the signal recognition particle: Binding of the two SRP protein heterodimers to SRP RNA is noncooperative. Biochemistry **31**, 5830–5840
25 Chang, D. Y., Newitt, J. A., Hsu, K., Bernstein, H. D. and Maraia, R. J. (1997) A highly conserved nucleotide in the *Alu* domain of SRP RNA mediates translation arrest through high affinity binding to SRP9/14. Nucleic Acids Res **25**, 1117–1122
26 Gowda, K., Black, S. D., Moeller, I., Sakakibara, Y., Liu, M.-C. and Zwieb, C. (1998) Protein SRP54 of human signal recognition particle: cloning, expression, and comparative analysis of functional sites. Gene **207**, 197–207
27 Huck, L., Scherrer, A., Terzi, L., Johnson, A. E., Bernstein, H. D., Cusack, S., Weichenrieder, O. and Strub, K. (2004) Conserved tertiary base pairing ensures proper RNA folding and efficient assembly of the signal recognition particle *Alu* domain. Nucleic Acids Res **32**, 4915–4924
28 Iakhiaeva, E., Yin, J. and Zwieb, C. (2005) Identification of an RNA-binding domain in human SRP72. J. Mol. Biol. **345**, 659–666
29 Iakhiaeva, E., Bhuiyan, S. H., Yin, J. and Zwieb, C. (2006) Protein SRP68 of human signal recognition particle: identification of the RNA and SRP72 binding domains. Protein Sci. **15**, 1290–1302
30 Lakkaraju, A. K., Mary, C., Scherrer, A., Johnson, A. E. and Strub, K. (2008) SRP keeps polypeptides translocation-competent by slowing translation to match limiting ER-targeting sites. Cell **133**, 440–451
31 Lutcke, H., Prehn, S., Ashford, A. J., Remus, M., Frank, R. and Dobberstein, B. (1993) Assembly of the 68- and 72-kD proteins of signal recognition particle with 7 S RNA. J. Cell Biol. **121**, 977–985
32 Thomas, Y., Bui, N. and Strub, K. (1997) A truncation in the 14 kDa protein of the signal recognition particle leads to tertiary structure changes in the RNA and abolishes the elongation arrest activity of the particle. Nucleic Acids Res. **25**, 1920–1929
33 Latham, J. A. and Cech, T. R. (1989) Defining the inside and outside of a catalytic RNA molecule. Science **245**, 276–282
34 Brenowitz, M., Chance, M. R., Dhavan, G. and Takamoto, K. (2002) Probing the structural dynamics of nucleic acids by quantitative time-resolved and equilibrium hydroxyl radical 'footprinting'. Curr. Opin. Struct. Biol. **12**, 648–653
35 Hainzl, T., Huang, S. and Sauer-Eriksson, A. E. (2002) Structure of the SRP19–RNA complex and implications for signal recognition particle assembly. Nature **417**, 767–771
36 Poritz, M. A., Strub, K. and Walter, P. (1988) Human SRP RNA and *E. coli* 4.5 S RNA contain a highly homologous structural domain. Cell **55**, 4–6

Received 12 March 2008/16 June 2008; accepted 18 June 2008
Published as BJ Immediate Publication 18 June 2008, doi:10.1042/BJ20080569